Auton Robot (2018) 42:1–17
https://doi.org/10.1007/s10514-017-9635-z

Robotic assembly solution by human-in-the-loop teaching method based on real-time stiffness modulation

Luka Peternel[1,2] · **Tadej Petrič**[1] · **Jan Babič**[1]

Received: 23 October 2015 / Accepted: 3 April 2017 / Published online: 12 April 2017

Abstract We propose a novel human-in-the-loop approach for teaching robots how to solve assembly tasks in unpredictable and unstructured environments. In the proposed method the human sensorimotor system is integrated into the robot control loop though a teleoperation setup. The approach combines a 3-DoF end-effector force feedback with an interface for modulation of the robot end-effector stiffness. When operating in unpredictable and unstructured environments, modulation of limb impedance is essential in terms of successful task execution, stability and safety. We developed a novel hand-held stiffness control interface that is controlled by the motion of the human finger. A teaching approach was then used to achieve autonomous robot operation. In the experiments, we analysed and solved two part-assembly tasks: sliding a bolt fitting inside a groove and driving a self-tapping screw into a material of unknown properties. We experimentally compared the proposed method to complementary robot learning methods and analysed the potential benefits of direct stiffness modulation in the force-feedback teleoperation.

Keywords Human-in-the-loop · Robot learning · Compliant assembly · Human–robot interface · Teleoperation

1 Introduction

Robots have been successfully integrated into the industrial and laboratory environments where they became indispensable tools in applications involving manipulation with the environment. There they can perform the designated tasks with unmatched operational speed and precision. However, to achieve the desired task execution, they are mostly pre-programmed manually by experts . This is a time-consuming process that usually requires precise modelling of the robot, environment and their interaction.

A convenient alternative to manual programming is using a robot learning approach. In one such promising instance, the robot autonomously learns the task based on the given cost function within the reinforcement learning framework (Theodorou et al. 2010; Kormushev et al. 2010; Buchli et al. 2011; Kober et al. 2012). The advantage of this method is that the robot can learn the task on its own. A potential drawback of this method is that the learning process is based on trail-by-error paradigm and requires some time for the robot to explore the space related to the task execution. This may hinder the method's applicability in industrial applications where we want the robot to learn a new task as quickly as possible to maximise its use. In addition, in the absence of human to supervise the learning process, trail-by-error approach may lead to a potential damage of expensive industrial equipment.

This work was supported by European Community Framework Programme 7 through the CoDyCo Project (Contract No. 600716).

Electronic supplementary material The online version of this article (doi:10.1007/s10514-017-9635-z) contains supplementary material, which is available to authorized users.

✉ Luka Peternel
luka.peternel@ijs.si; luka.peternel@iit.it

Tadej Petrič
tadej.petric@ijs.si

Jan Babič
jan.babic@ijs.si

[1] Department of Automation Biocybernetics and Robotics, Jožef Stefan Institute, Jamova cesta 39, 1000 Ljubljana, Slovenia

[2] HRII Lab, Department of Advanced Robotics, Istituto Italiano di Technologia, Via Morego 30, 16163 Genoa, Italy

An alternative to reinforcement learning is learning by demonstration where the human simply demonstrates the skill to the robot (Billard et al. 2008; Argall et al. 2009). This framework requires a constant presence of the human during the entire learning process. However, the robot can potentially learn new tasks faster and safer, which makes it suitable for industrial environment. One of the most common learning-by-demonstration approaches is kinaesthetic teaching where the human demonstrates the execution of the task by physically holding and manipulating the robot (Kushida et al. 2001; Hersch et al. 2008; Ben Amor et al. 2009; Calinon et al. 2010; Lee and Ott 2011; Kormushev et al. 2011; Kronander and Billard 2014). The practical nature of this approach makes it very convenient and intuitive. However, it can have several drawbacks such as: the inability of human to teach the robot remotely in cases of operation in hazardous environments; difficulty to simultaneously control the impedance of the robot (Hogan 1985); and demonstrator-induced dynamics during the teaching stage, which may alter the dynamical conditions between the demonstration and the autonomous stages.

A solution to these drawbacks is to teach the robot through teleoperation where the human demonstrator is not physically coupled with the robot during the demonstration stage. To transfer the motion to the robot and to provide force feedback to the human during the teaching process, the human can be included into the robot control loop by various haptic interfaces such as hand-held devices (Evrard et al. 2009; Walker et al. 2011; Kormushev et al. 2011) that allow teaching of various manipulation tasks. In some cases, the teleoperation (Ajoudani et al. 2012) or teaching through teleoperation (Peternel et al. 2014) can be successfully performed without providing the demonstrator with a feedback about the forces measured between the robot end-effector and the environment. Instead, these approaches rely on a combination of visual feedback and the ability of the teleoperator to modulate the impedance of the robot.[1]

Currently, industrial robots mainly operate at preset high impedance where a precise model of the task is required to achieve the desired physical interaction. However, if the robot operates in an unstructured environment then the models of the task are not available. Modelling becomes even more complicated when the robot or the environment are subject to unpredictable events and external perturbations. Despite these difficulties, humans are able to successfully operate the robot in such environments. One of the key properties that allow us to simplify physical interaction with the environment is the ability to adapt the end-point impedance our limb through a coordinated function of muscles (Burdet et al. 2001). This is possible due to the spring-like property of the muscles and the redundancy provided by the antagonist muscle pairs that enable the control of joint stiffness independently of the joint torque (Hogan 1984). Inspired by the advantages of human arm impedance control, researchers have proposed to control the robot arm impedance either algorithmically (Hogan 1985; Albu-Schäffer et al. 2007; Schindlbeck and Haddadin 2015), by using clutches (Walker et al. 2010) or by using variable stiffness actuators (Tonietti et al. 2005; Wolf and Hirzinger 2008).

There are numerous occasions where arm impedance has to be adjusted to achieve the desired task execution. One of the most prominent examples is to approach the unstructured environment with a lower impedance to prevent high impact forces at the time of initial contact (Walker et al. 2010, 2011; Ajoudani et al. 2012; Schindlbeck and Haddadin 2015). On the other hand, if the limb operates within the unstable environment, the impedance should be increased to achieve the expected robustness and accuracy (Burdet et al. 2001; Yang et al. 2011). The use of variable impedance can also maximise energy efficiency of the manipulator in tasks such as object throwing (Wolf and Hirzinger 2008; Walker et al. 2011) and nail hammering (Garabini et al. 2011). Furthermore, adjustments of arm impedance can simplify the execution of tasks where two agents have to cooperate with each other (Tsumugiwa et al. 2002; Peternel et al. 2014; Rozo et al. 2015; Peternel et al. 2016b). In addition, low impedance motion makes the robot much safer when humans intersect its workspace (De Luca et al. 2006). This is particularly important during human–robot cooperation where the human behaviour is unpredictable (Peternel et al. 2014, 2016b).

1.1 Related work

Some researchers (Calinon et al. 2010; Lee and Ott 2011; Kormushev et al. 2011; Paraschos et al. 2013) proposed to use the variability of human-demonstrated motion trajectories to estimate the robot impedance. They hypothesised that a small variability in motion should correspond to a higher tracking precision and therefore to a higher robot stiffness to maintain that precision, and vice-versa. In a similar instance, an optimal feedback controller was used to govern the impedance of the demonstrated probabilistic behaviour (Rozo et al. 2015). In the above-mentioned approaches the human has no direct control over the impedance, which can in some cases lead to an undesirable behaviour (see Sect. 3.1 for analysis).

In another approach, the demonstrator directly alters the impedance of the robot trough the kinaesthetic interaction (Kronander and Billard 2012, 2014). The impedance is decreased by wiggling the robotic limb around the demonstrated position, or increased by producing a grip force on the robot (Kronander and Billard 2014). However, this approach inherits previously mentioned limitations of the

[1] For the sake of generality of introduction we use term "modulation of the impedance" when either stiffness, damping or mass is modulated in real time.

kinaesthetic guidance. Yang et al. (2011) proposed a human-like inspired impedance controller that gradually updates the stiffness to minimise the effort and the motion error due to the disturbances in the environment. Buchli et al. (2011) proposed a solution for learning robot impedance where they used path-integral based reinforcement learning not only for the planning but also to derive variable-gain feedback controllers in realistic scenarios. Iterative learning process can be time-consuming and in some applications impractical. Furthermore, the potential of using human sensorimotor and cognitive abilities to directly transfer the skill to the robot is missing. In the absence of human supervision, the approach may also lead to damage of expensive industrial equipment.

Some studies proposed methods to control the impedance in teleoperation setup directly in real-time [this principle is sometime referred to as "tele-impedance" (Ajoudani et al. 2012)]. (Ajoudani et al. 2012) proposed a method to estimate the impedance of the teleoperator's arm end-effector based on the human muscle activity patterns and transfer it to the robotic arm end-effector. Peternel et al. (2014) proposed a simplified single-muscle impedance control interface for robot teaching trough tele-impedance. These methods do not provide the teleoperator with the force feedback. Nevertheless, it has been demonstrated that it is sometimes sufficient to modulate the robot impedance in real-time by simple visual feedback (Ajoudani et al. 2012; Peternel et al. 2014).

However, force feedback at the teleoperator's end-effector can provide additional information about the robot's state and improve the immersion of the operator. Nevertheless, this can introduce several stability issues as the applied feedback force induces undesired commanded end-effector motion (Hannaford and Anderson 1988; Kuchenbecker and Niemeyer 2006). A few studies explored the use of force feedback in a combination with the direct impedance modulation. Tactile squeezing and vibrating devices can be used to provide additional feedback about the robot force without influencing the human arm end-effector motion (Ajoudani et al. 2014). This method bypasses the above-mentioned instability at the expense of losing the direct force feedback at the end-effector. A study by (Walker et al. 2010) used force feedback at the end-effector of the haptic interface with a combination of the stiffness modulation interface. However, their study was limited to a simple 1-DoF feedback.

1.2 Paper contributions

The contributions of this paper are: (1) human-in-the-loop robot teaching method that combines direct control of the robot end-effector stiffness with the 3-DoF end-effector force feedback, (2) hand-held stiffness control interface controlled by the human finger, (3) analysis of potential benefits of the human's ability to directly control the stiffness with respect to the force-feedback teleoperation stability, and (4) experimental analysis and comparison of the proposed method in two robotic assembly tasks.

To complement the impedance teaching methods based on either kinaesthetic interaction (Kronander and Billard 2014), variability in demonstrated motion (Calinon et al. 2010; Lee and Ott 2011; Kormushev et al. 2011; Paraschos et al. 2013; Rozo et al. 2015) or iterative improvements (Yang et al. 2011; Buchli et al. 2011), we propose a novel robot teaching method based on teleoperation of the robot in real-time, where the operator can directly demonstrate the stiffness. The novelty of the proposed approach, compared to the above-mentioned approaches, is that the human demonstrator has a direct control over the demonstrated impedance strategy. We demonstrate this advantage by experimental and comparative analyses (see Sect. 3.1).

To improve the human's immersion in classical tele-impedance (Ajoudani et al. 2012; Peternel et al. 2014), we introduce a 3-DoF force feedback at the tutor's[2] end-effector. A haptic interface is used to measure the position of the tutor's arm end-effector and provides a 3-DoF force feedback at the same time. The classical teleoperation setup is enhanced by a novel stiffness control interface that allows the tutor to modulate the robot stiffness in real-time according to the task demands. We propose and analyse the possibility to stabilise the force-feedback teleoperation using the proposed method (see Sect. 2.3).

The main advantage of the proposed method is that it provides easy and fast means to relay new skills to the robot. The human can simply teach the robotic arm how to perform a complex task through operating it in real-time. Compared to the manual programming, the desired motion of the robot can be generated much faster as the motion points are demonstrated in real-time at high sampling rate. Demonstrating the force-control skill with manual programming techniques requires precise models of the environment. Using our approach, the desired force-level skill can be efficiently demonstrated through the proposed interface without the need to model the environment. Instead, the human generates the desired robot behaviour based on his/her sensorimotor and cognitive capabilities.

The proposed framework is intended for teaching the robots how to physically interact with the environment and execute various manipulation tasks. To demonstrate the applicability of the proposed approach, we performed experiments on KUKA *Lightweight Robot* arm and taught the robot how to perform several challenging assembly tasks. Specifically, we analysed strategies of two tasks: part assembly by attaching bolt fitting inside a groove and by using self-tapping bolts.

A preliminary study was presented at 2015 *IEEE/RAS International Conference on Automation and Robotics*

[2] Tutor is a teleoperator that teaches the robot a new behaviour.

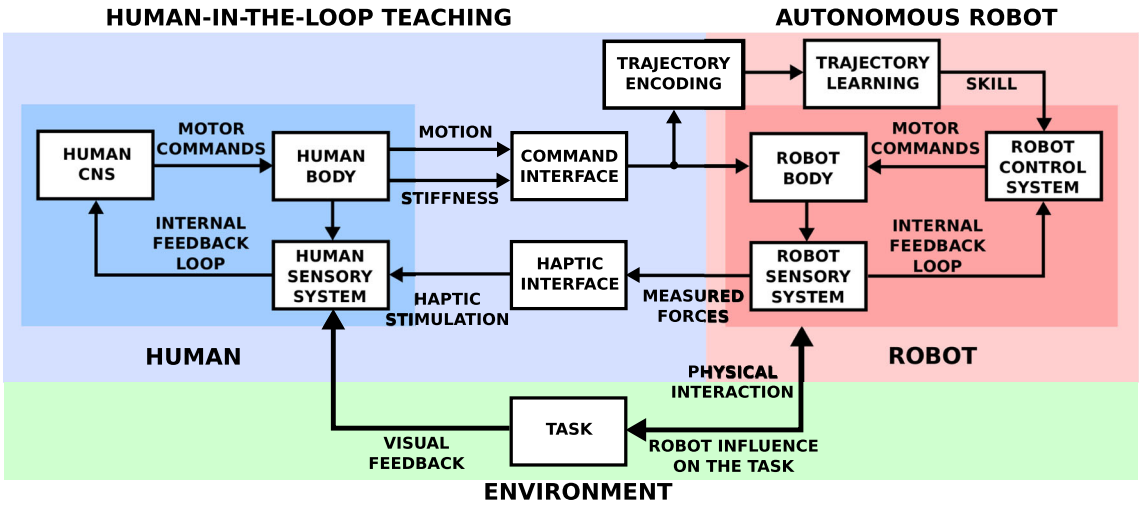

Fig. 1 Block diagram of proposed human-in-the-loop robot teaching framework. During the demonstration stage the human tutor is operating and teaching the robot (*blue* section). When the learning process is completed the robot reproduces the demonstrated skill autonomously (*red* section) (Color figure online)

(Peternel et al. 2015). In this paper we expanded the state-of-the-art review and method formulation. We added novel experimental analyses, comparison and results. We examined a solution of an additional task that involves robotic screwing of self-tapping bolt into a material of unknown properties. We added an analysis regarding potential benefits of the tutor's ability to directly control the impedance with respect to the force-feedback teleoperation stability.

2 Methods

The block diagram of the proposed robot teaching method is shown in Fig. 1. The tutor was included into the robot control loop through a haptic feedback interface on one side and through motion/stiffness control interface on the other side. The proposed method is based on utilisation of the sensorimotor learning ability of the human tutor. Specifically, human central nervous system (CNS) is capable of learning various complex tasks and tool use (Imamizu et al. 2000). It has been argued that our CNS is able to acquire and hold internal models of external world, which allows us to perform various sensorimotor-level tasks (Wolpert et al. 1998; Kawato 1999). We are able to include external objects such as tools into our body schema and operate them as if they were a part of our body. In the same sense, the human CNS can perceive the teleoperated robot as a tool and include it into the body schema (Oztop et al. 2006; Babič et al. 2011; Peternel et al. 2014). When the tutor obtained the necessary skill to perform the task by the robot, we collected the data related to the motor control during the given conditions. The data was then used to transfer the obtained human skill into the robot control system that enables the robot to perform the task autonomously. It is important to note that the learnt robot skill is primarily suitable for the robot. The obtained skill itself might not necessarily be human-like as the human demonstrator primarily adapts to optimise the control of a novel system (i.e. robotic limb).

In each experiment, we first gave the tutor the time necessary to adapt to the robot through sensorimotor learning. Meanwhile, the human used cognitive capabilities to devise the strategy for task solution. We then proceeded to the teaching stage where the trained tutor operated the robot by commanding both the desired motion and the stiffness of the robotic arm. The motion of the human arm was measured by a haptic device [Moog *HapticMaster* robot (Van Der Linde et al. 2002)] and was sent to the robot end-effector in real-time. The forces exchanged between the robot end-effector and the environment were measured by the robot sensory system and were fed back to the human through a haptic device. At the same time, the tutor used visual feedback to determine the actual position and motion of the robotic arm. During the demonstration stage, the learning system stored the motor control data related to the task execution (i.e. motion and stiffness).

The collected data was then used to generate trajectories of the robot end-effector motion and stiffness, which were then used to execute the task autonomously. To encode the trajectories we used Dynamical Movement Primitives (DMPs) (Ijspeert et al. 2002a, b) that have been previously successfully applied in various robot learning techniques (Kormushev et al. 2010; Peternel et al. 2014; Ben Amor et al. 2014; Peternel et al. 2016a). We chose DMPs because they are easy-to-use and offer many good properties: they are robust to perturbations, not explicitly time-dependant, can be easily learnt and modulated on-line,

etc. (Ijspeert et al. 2013), and can be easily coupled with adaptive oscillators to control their execution frequency and phase (Petrič et al. 2011; Peternel et al. 2014, 2016a).

With the proposed approach we aim to teach industrial robots various interaction tasks. Since the majority of industrial tasks are of repetitive nature, we chose to use periodic DMPs (Ijspeert et al. 2002a) to encode these actions. However, the proposed approach is not limited to periodic motion. Point-to-point DMPs (Ijspeert et al. 2002b) can be used as well. The trajectories were normalised with respect to the phase of the periodic cycle, which allowed us to arbitrary slow down or speed up the different sections of the cycle. In addition, we were able to stop the operation at some predefined phase in order to make additional action such as tightening the bolt in the assembly task.

2.1 Trajectory learning system

Here we give a short recap of DMPs. They are based on a second order system of differential equations (Ijspeert et al. 2002b)

$$\dot{b} = \Omega\left(\alpha\left(\beta\left(-a\right) - b\right) + f\right), \tag{1}$$

$$\dot{a} = \Omega b, \tag{2}$$

where a is the trajectory, Ω is the frequency, f is the nonlinear shape function, which alters the second order differential equation, and α and β are positive constants. Gaussian kernels are used to produce shape f

$$f(\phi) = \frac{\sum_{i=1}^{N} \psi_i(\phi) w_i}{\sum_{i=1}^{N} \psi_i(\phi)}, \tag{3}$$

where w_i are weights and $\psi_i(\phi)$ are phase-dependant Gaussian kernels defined as

$$\psi_i(\phi) = e^{h(\cos(\phi - c_i) - 1)}, \tag{4}$$

where parameter h is the width of the Gaussian kernel, c_i are the uniformly distributed centres of the kernels across the phase (between 0 and 2π), and N is the number of weights. Number of weights determines the desired resolution of trajectory. For our experiments we selected 50 weights.

Locally Weighted Regression (Schaal and Atkeson 1998) was used to learn the shape function f by the following approximation

$$f_d = \frac{\ddot{p}_d}{\Omega^2} - \alpha\left(\beta\left(-p_d\right) - \frac{\dot{p}_d}{\Omega}\right), \tag{5}$$

where p_d, $\dot{p}_d$ and $\ddot{p}_d$ are either the demonstrated commanded motion or stiffness and their derivatives. The equation is given for one DOF. For multiple DOFs they can be used in parallel. Weights w_i of Gaussian kernel functions ψ_i are updated using a recursive least squares method with forgetting factor λ (Schaal and Atkeson 1998)

$$w_i(t+1) = w_i(t) + \psi_i P_i(t+1) r e_r(t), \tag{6}$$

$$e_r(t) = f_d(t) - w_i(t) r, \tag{7}$$

$$P_i(t+1) = \frac{1}{\lambda}\left(P_i(t) - \frac{P_i(t)^2 r^2}{\frac{\lambda}{\psi_i} + P_i(t) r^2}\right), \tag{8}$$

where the parameters were initially set as $w_i(0) = 0$, $P_i(0) = 1$, $i = 1, 2, \ldots, N$. For the purpose of our experiments we selected $\lambda = 0.99995$.

To control the phase of the learnt trajectories we used the sawtooth wave generated by

$$\dot{\phi} = \Omega = \frac{2\pi}{T}, \tag{9}$$

where Ω is the desired reproduction frequency and T is the desired period. The trajectory execution can be temporary stopped at a desired phase by setting the frequency to zero.

2.2 Robot stiffness control interface

Impedance control interfaces that are based on human muscle activity were shown to be very effective in tele-impedance (Ajoudani et al. 2012; Peternel et al. 2014; Liang et al. 2015). However, they require time-consuming calibration procedures and knowledge of the human anatomy, which can make them less suitable for the industrial application. An interface based on hand grip force was proposed by Walker et al. (2010) but the regulation of the hand grip force may not be trivial (Todd et al. 2010; Emge et al. 2013).

As an alternative to the above-mentioned methods, we propose a novel impedance control interface for robot teaching (see Fig. 2). This interface uses a spring-return linear potentiometer mounted inside a handle that is held by the tutor. The tutor uses index finger to control the position of the potentiometer. This setup retains the simplicity and applicability of the grip-force interface (Walker et al. 2010), while the finger position based input requires little effort from the tutor. In addition, the potentiometer is a low-cost device compared to a grip-force sensor.

The potentiometer voltage related to finger position was read with AD converter and mapped to the robot end-effector stiffness. We first acquired the stiffness modulation vector from the potentiometer

$$\boldsymbol{c} = \frac{V(t)^2}{V_{max}^2}\left(\boldsymbol{k}_{max} - \boldsymbol{k}_{min}\right) + \boldsymbol{k}_{min}, \tag{10}$$

where $\boldsymbol{c}$ is a vector used to modulate the stiffness of the robot, $V(t)$ is the potentiometer voltage at time t and V_{max}

Fig. 2 Robot control interface consisting of *HapticMaster* robot and stiffness control handle. *HapticMaster* robot measures the commanded position and provide the force feedback. The tutor holds the stiffness control handle that contains a spring-return linear potentiometer

is the maximum voltage. Vectors $\boldsymbol{k}_{max}$ and $\boldsymbol{k}_{min}$ are used to determine the controllable stiffness range and are composed of the positional and rotational components. To keep the i-th axis stiffness unaffected by the interface, $\boldsymbol{k}_{max}(i) = 0$ and $\boldsymbol{k}_{min}(i) = 0$ should be used. As opposed to Peternel et al. (2014), where a linear mapping was used, we used a quadratic mapping to give more sensitivity to the low-stiffness section of the range. Robot Cartesian stiffness was controlled by

$$\boldsymbol{k} = \boldsymbol{c} + \boldsymbol{o}, \tag{11}$$

$$\boldsymbol{k} = [\boldsymbol{k}^{pos}\ \boldsymbol{k}^{rot}], \tag{12}$$

where $\boldsymbol{k}$ is a vector containing the desired Cartesian stiffness parameters composed of positional $\boldsymbol{k}^{pos}$ and rotational $\boldsymbol{k}^{rot}$ components. Vector $\boldsymbol{o}$ is used if we wish to keep i-th axis at some preset constant stiffness when $\boldsymbol{k}_{max}(i) = 0$ and $\boldsymbol{k}_{min}(i) = 0$. The parameters $\boldsymbol{k}$ were used as an input for robot Cartesian impedance controller (Albu-Schäffer et al. 2007).

We altered the robot impedance by changing the stiffness term in the robot impedance control scheme. The force that the robot exerts on an external object is generated by moving the reference (commanded) position inside the object to achieve a displacement between the actual robot position (blocked by the object surface) and reference position inside the object. The desired interaction force/torque is defined as (Hogan 1985)

$$\boldsymbol{F}_{ext} = \boldsymbol{K}\left(\boldsymbol{x}_d - \boldsymbol{x}_a\right) + \boldsymbol{B}\left(\dot{\boldsymbol{x}}_d - \dot{\boldsymbol{x}}_a\right), \tag{13}$$

where $\boldsymbol{F}_{ext}$ is the Cartesian space interaction force/torque acting from the robot on the environment, $\boldsymbol{K} = \text{diag}(\boldsymbol{k})$ and $\boldsymbol{B}$ are the robot virtual stiffness and damping matrices in Cartesian space, $\boldsymbol{x}_a$ is the actual and $\boldsymbol{x}_d$ is the reference pose of the robot end-effector. The actual pose $\boldsymbol{x}_a$ also depends on the environment. The desired interaction force in Cartesian space was controlled at the robot joint torque level

$$\boldsymbol{M}(\boldsymbol{q})\ddot{\boldsymbol{q}} + \boldsymbol{C}(\boldsymbol{q}, \dot{\boldsymbol{q}})\dot{\boldsymbol{q}} + \boldsymbol{g}(\boldsymbol{q}) = \boldsymbol{\tau} - \boldsymbol{J}^T \boldsymbol{F}_{ext}, \tag{14}$$

where $\boldsymbol{\tau}$ is a vector of robot joint torques, $\boldsymbol{q}$ is a vector of joint angles, $\boldsymbol{J}$ is the robot Jacobian matrix, $\boldsymbol{M}$ is the mass matrix, $\boldsymbol{C}$ is Coriolis and centrifugal vector and $\boldsymbol{g}$ is the gravity vector. Given that we know the dynamical model of the robot, we can calculate the necessary joint torques $\boldsymbol{\tau}$ to produce the desired interaction force/torque $\boldsymbol{F}_{ext}$.

The desired force that the robot exerts on the environment can be achieved by different combinations of the desired end-effector position and stiffness. This redundancy provides many task-related benefits, which were mentioned in the introduction. On the other hand, the ability to command the robot impedance can provide several additional teaching-level benefits. It is well known that the feedback-force induced motion at the human end-effector, combined with the delays in the teleoperation loop, can destabilise the teleoperator's arm and cause oscillations (Kuchenbecker and Niemeyer 2006). Using the proposed approach, the tutor can exploit the ability to directly control the stiffness to minimise the instability of teleoperation setup related to the force-feedback.

2.3 Analysis of potential force feedback stabilisation

Applying 3-DoF feedback force at the human arm end-effector in the teleoperation setup is important as it relays a direct information about the robot contact with environment. However, it can introduce some challenges. The transmission delays in the system loop and delays in human neural feedback loops may cause stability problems. The feedback force exerted on tutor's arm end-effector induces undesirable motion of the tutor's arm which is reflected on the robot side through the altered commanded motion (Hannaford and Anderson 1988; Kuchenbecker and Niemeyer 2006). This effect can produce oscillation in the movement of the robot. The actual commanded robot position is the sum of motion commanded by the tutor and the undesirable motion from the feedback force (Kuchenbecker and Niemeyer 2006)

$$\boldsymbol{x}_d(t + t_s) = \boldsymbol{x}_{FF}(t) + \boldsymbol{x}_{FB}(t), \tag{15}$$

where t is the current time, t_s is a sample time, $\boldsymbol{x}_d$ is the actual commanded robot position, $\boldsymbol{x}_{FF}$ is the intended/desired commanded position and $\boldsymbol{x}_{FB}$ is the force feedback induced motion which is equal to (Kuchenbecker and Niemeyer 2006)

$$\boldsymbol{x}_{FB}(t) = \mathcal{D}\big(-K_{FB}\boldsymbol{F}_r(t)\big), \tag{16}$$

$$\boldsymbol{F}_r = \boldsymbol{K}\big(K_{FF}\boldsymbol{x}_d(t) - \boldsymbol{x}_a(t)\big), \tag{17}$$

where $\mathcal{D}$ represents the combined dynamics of tutor arm and the haptic device, $\boldsymbol{F}_r$ is the force produced by the robot, $\boldsymbol{K}$ is Cartesian stiffness matrix of the robot impedance control scheme, $\boldsymbol{x}_d(t)$ is the commanded and $\boldsymbol{x}_a(t)$ is the actual robot position at the current time t, while K_{FF} and K_{FB} are feed-forward position and feedback force scaling factors of teleoperation setup. Since we use 3-DoF force feedback in the proposed method we limit this analysis to the positional components of Cartesian space.

Stability in the force-feedback teleoperation can be achieved by several methods. The tutor can voluntarily increase the impedance of his/her arm end-point by co-activating the muscles. Different co-activation of antagonist muscle pairs yields different stiffness in the corresponding joints due to the spring-like properties of human muscles (Hogan 1984). On a single joint level, the higher the muscle co-activation, the smaller the displacement due to an external perturbation force. The human can generalise this to a multi-joint level by co-activating the arm muscles to control the impedance of the arm end-point (Burdet et al. 2001). Such stabilisation approach may be effective to some degree but it demands a considerable physical effort from the teleoperator/tutor.

A more convenient approach for achieving a stable teleoperation is by using various software solutions. One such approach exploits the values of feed-forward position scaling factor or force feedback scaling factor (Kuchenbecker and Niemeyer 2006). If lower feed-forward scaling factor is used then the induced motion on the tutor's side produces smaller undesirable motion on the robot side. On the other hand, low feedback factor scales down the feedback force that can potentially destabilise the tutor's arm (Kuchenbecker and Niemeyer 2006). However, the scaling factors cannot always be freely selected and are highly dependant on the hardware and the task.

Hannaford and Anderson (1988) proposed adding the damping term to the internal loop of the master device, which filters force feedback from high motion velocity. However, this requires clean measurement of velocities and may make the system unresponsive due to the damping. Another approach is based on low-pass filtering of commanded position signal (Fite et al. 2001). This approach is easy to implement but the filtering limits the frequency of the motion that can be transferred from the human to the robot. Alternatively, force feedback signal can be filtered to prevent rapid changes of the force applied to the human arm (Daniel and McAree 1998), but the reproduced force frequency range is limited. Kuchenbecker and Niemeyer (2006) proposed an approach to cancel the induced motion by using the model of relation between feedback and induced motion.

In this paper, we analyse a potential approach to stabilise the force-feedback teleoperation by the tutor's ability to control the robot arm impedance in real-time. If the tutor has the ability to alter the robot stiffness and motion, this introduces a redundancy in the robot force control. In theory, the same force can be achieved with infinite combinations of the stiffness and the error between the referent and the actual robot position (see Fig. 3, right graph). By changing the stiffness of the robot end-effector, the tutor can scale the sensitivity of the force feedback variation to the variation in the commanded position that results from the induced feedback

$$\Delta\boldsymbol{F}_r(t) = \boldsymbol{K}(tutor)\big(K_{FF}\Delta\boldsymbol{x}_d(t) - \boldsymbol{x}_a(t)\big), \tag{18}$$

where $\boldsymbol{K}(tutor)$ signifies the robot stiffness that can be modulated by the tutor.

A similar approach to stabilise the teleoperation was proposed by Kim et al. (1992). They designed a selective compliant control that includes a low-pass filter in the robot internal control loop. By changing the parameters of the filter the compliance of the robot can be increased, which in turn stabilises the teleoperation loop. However, this approach requires manual tuning of the parameter off-line and is limited to the selection of several predefined parameters.

On the other hand, using the proposed stiffness control interface, the tutor can control the robot virtual stiffness parameter $\boldsymbol{K}(tutor)$ directly and continuously across its range in real-time. Consequently, he/she can modulate the relation between the output force $\boldsymbol{F}_r$ and the displacement of the commanded position from the actual position. The difference between the robot commanded and the actual position must be higher at a low gain $\boldsymbol{K}(tutor)$ to achieve the same robot force when the gain $\boldsymbol{K}(tutor)$ is high. By observing (18), we can see that the variation in the commanded robot position due to the force-feedback induced motion $\boldsymbol{x}_{FB}$ has much smaller effect on the variation of the robot force when commanding with a low gain $\boldsymbol{K}(tutor)$.

We must note that this human-controlled stabilisation solution can only be applied if the task does not impose the constraint on the variability of the stiffness within this redundant force control concept. For example, if the task specifically requires a relatively high stiffness then the redundancy in force control is constrained within some region that may have potential destabilising effect on the teleoperation framework. In this case, the teleoperation should be stabilised by one of the aforementioned approaches that does not alter the robot compliance.

We performed a force-production task experiments to analyse the proposed interface and demonstrate the effects of controllable robot stiffness on the force-feedback induced motion. A trained tutor was asked to produce three differ-

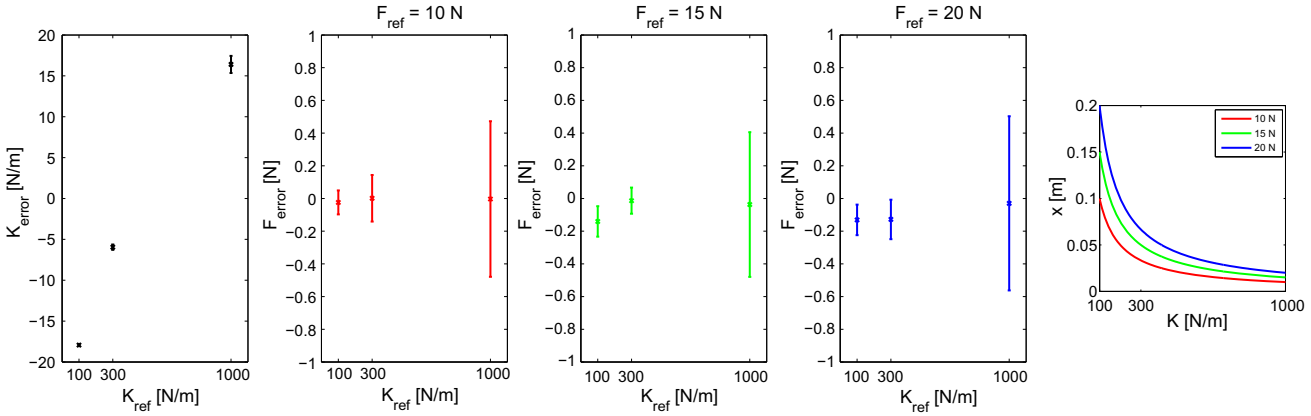

Fig. 3 Result of force production experiment. The *left-most graph* shows the tutor's error in maintaining the reference stiffness using the proposed interface. The *middle three graphs* show the robot produced force error in *z-axis* for different reference forces (10, 15, 20 N) and different reference commanded stiffness (100, 300, 1000 N/m). The *middle point* of each *bar* corresponds to the mean error and the height of the *bar* corresponds to the standard deviation of the sampled data over the observation interval in each reference conditions. The *right-most graph* shows the theoretical relation between the input parameters (difference between reference and commanded position, and commanded stiffness) and output parameter (produced force)

ent forces (10, 15, 20 N) perpendicularly to the environment (z-axis) by commanding three different robot stiffness values (100, 300, 1000 N/m). Figure 3 shows the result of the experimental analysis. We can see that the actual produced force varied a lot more when the tutor commanded a higher stiffness (1000 N/m). On the other hand, the tutor could maintain the desired force with considerably less variation at lower commanded stiffness (100 and 300 N/m). The observed behaviour is in accordance with (18) and is further highlighted by the right-most graph. Variation of commanded position has less affect on force variation when lower stiffness is commanded.

3 Experiments

One of the common industrial tasks is an assembly of an object from several parts that may involve various elementary sub-tasks, which require adaptation of robot arm impedance for simplified and safe execution. Peg-in-the-hole task is one such example that has been extensively studied in the past (Tsumugiwa et al. 2002; Ajoudani et al. 2012; Walker et al. 2011; Kronander et al. 2014). The usual strategy for solving the peg-in-the-hole task is to first approach the hole with a low impedance in order to reduce the force of the impact and allow the peg to fit into the hole, and then increase the impedance to push the peg inside a tight spot.

In this paper, we used the proposed approach to solve two complementary assembly tasks. In the first case we focused on an elementary task that involved fixing two parts together with a bolt fitting. This task required the robot to insert a bolt fitting inside a groove of the complementary part and then slide it to a position where the bolt is to be fixed and hold the two parts together (see Fig. 4). In the second case we focused on using a self-tapping screw to fix parts. The Cartesian stiffness parameters $\boldsymbol{k}$ were set for each experiment separately based on the task requirements. The damping factors of the Cartesian damping design (Albu-Schäffer et al. 2003) were set in both experiments to $\xi = 0.7$.

3.1 Silde-in-the-grove task

We designed a strategy to solve the slide-in-the groove task that included three main segments (see Fig. 4): moving the part in the air, bolt insertion, and sliding the bolt inside the groove. Each segment was determined by the phase variable ϕ. In the first segment, the tutor increased the stiffness of the robotic arm when it was moving the part in air, in order to provide the high tracking precision in case of potential external disturbances (Burdet et al. 2001).[3] This strategy is not intended to solve collisions but rather to make the robot stable in its intended path. In case of collision possibilities or human–robot cooperation the stiffness should be kept at a lower level during this phase.

When the robot approached the groove insertion point in the second segment of the task, the tutor lowered the stiffness to minimise the impact forces (Walker et al. 2011; Ajoudani et al. 2012), but at the same time kept it high enough to maintain the tracking precision required for the insertion of the bolt. While sliding towards the fixation position during the third segment of the task, the tutor kept the stiffness low

[3] Note that the strategies are devised for autonomous robot operation and not for the comfort of the tutor during the teaching stage.

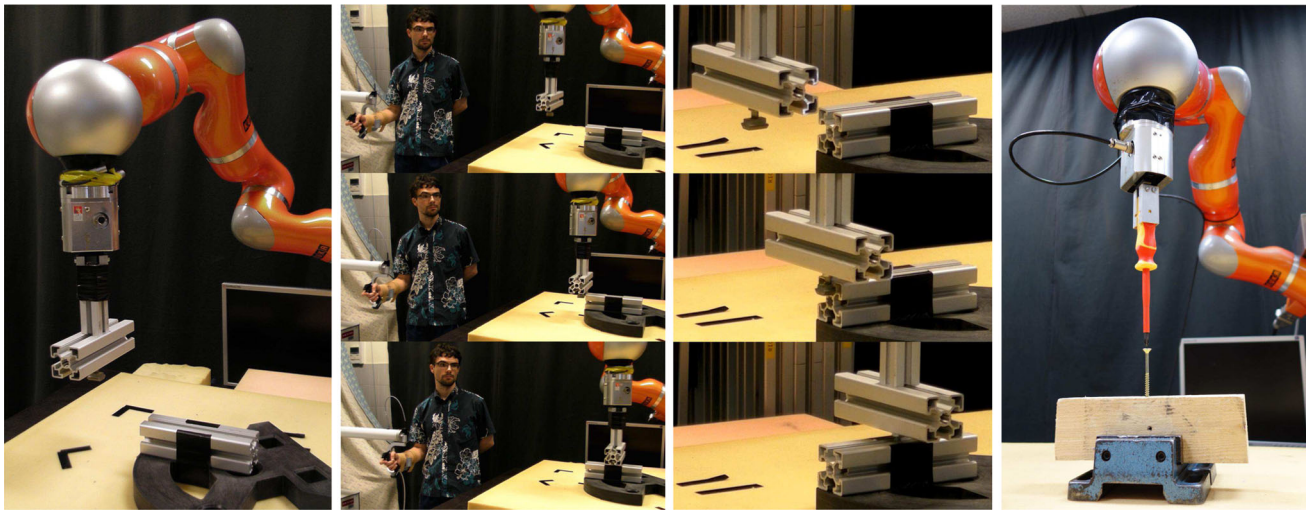

Fig. 4 Experimental setups for slide-in-the-groove assembly task (*left* and *middle* photos) and bolt-screwing task (*right* photo). The sequence of photos in the *second column* shows the human-in-the-loop teaching stage. The sequence of photos in the *third column* shows the autonomous robot operation of the learnt task

as the rigid environment itself (i.e. the groove) provided the necessary stabilisation for the robot. At the same time, low stiffness provided a preventive strategy against the unpredictable events. For example, if the base part with the groove moves when the robot stiffness is high, it produces high forces between the bolt fitting and the groove. Such events may potentially make the bolt stuck or even damage the equipment.

The stiffness control interface parameters were set as follows: maximum positional stiffness to 2000 N/m, minimum positional stiffness to 0 N/m for all three axes and constant rotational stiffness to 200 Nm/rad for all three axes. A trained tutor was instructed to teach the robot how to perform the given slide-in-the-groove task according to the designed strategy. During the teaching procedure we collected training data consisting of commanded robot end-effector position and stiffness. After the demonstration stage, we proceeded to the robot learning stage where the data was used to form trajectories, which were normalised to phase and encoded with periodic DMPs. The course of the teaching stage is shown in the second column photos of Fig. 4. Online Resource 1 accompanying this paper contains a video of this experiment.

Left column graphs of Fig. 5 show the trajectories formed from the demonstrated data (blue lines) and their corresponding DMPs (red lines) using the proposed human-in-the-loop approach. The first graph shows the trajectory of motion in y-axis, while the second graph shows the motion in z-axis of to the world reference frame. The y-axis of the world reference frame roughly coincided with the groove of the base part. The x-axis was perpendicular to the groove. The z-axis was in the opposite direction of gravity. The last graph shows the stiffness of the robot end-effector as it was modulated directly by tutor.

As a comparison we used the inverse of variability of motion trajectories sampled from multiple demonstrations (15 trials) to obtain the desired robot stiffness for each task segment (see Fig. 5 right column), which conceptually corresponds to the approaches proposed by Calinon et al. (2010), Lee and Ott (2011), Kormushev et al. (2011) and Paraschos et al. (2013). The same controllable stiffness range was used as in the proposed human-in-the-loop approach. We observed the trajectories in x-axis, as this is the axis that is the most susceptible to the external perturbations. We can see that the stiffness strategies (trajectories) obtained by the proposed approach and by the variability-based approach are inverted. Using the proposed approach, we can see that the tutor could use its cognitive capabilities to form a suitable robot strategy for the given task and then demonstrate it directly.

On the other hand, variability-based approach is limited to the variability of the demonstrated trajectories. Strategy obtained by the variability-based approach would command high stiffness during the bolt-insertion segment (around phase 0.4–0.5), where the robot should ideally approach the environment with lower stiffness. More importantly, the commanded stiffness obtained by the variability-based approach inside the groove (phase 0.5–0.8) was high. This was because the robot end-effector (bolt) was constrained by the environment (groove) and therefore the variation of the demonstrated trajectories was naturally low. However, the strategy should ideally command low robot stiffness when the bolt is inside the groove to avoid excessive forces in case of external perturbations. In addition, when the bolt was inside the groove, the environment already provided the stabilisation and therefore

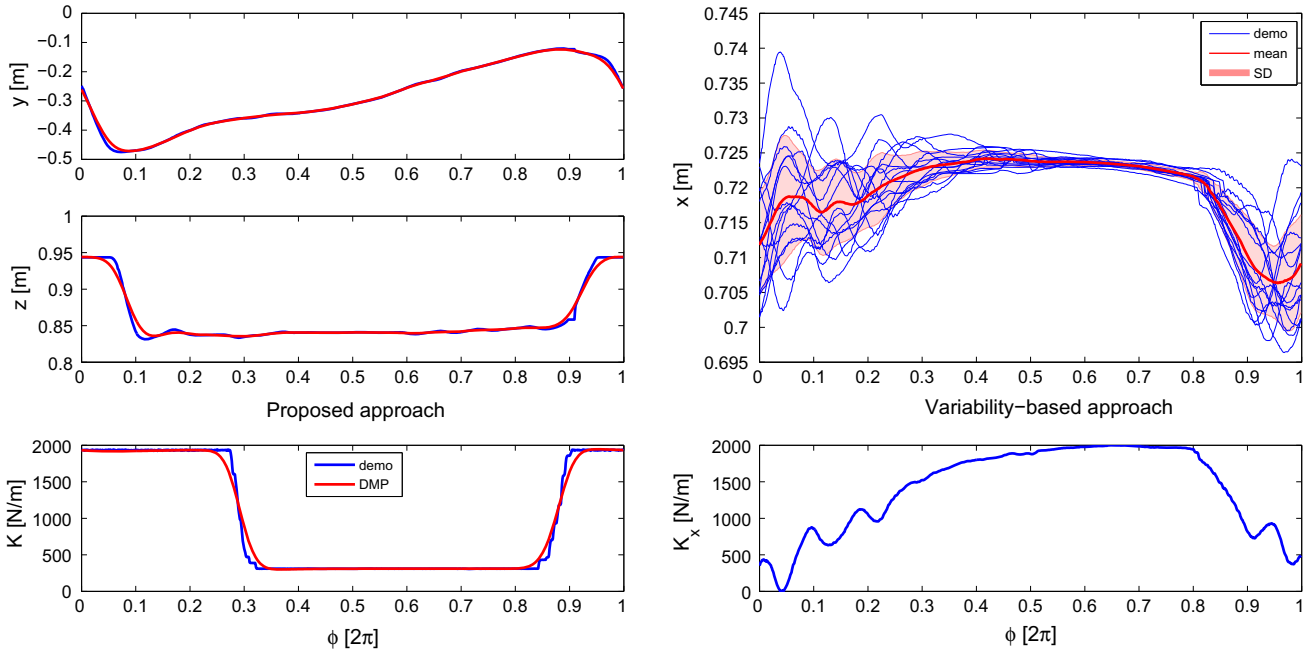

Fig. 5 Result of slide-in-the-groove assembly task teaching using the proposed approach (*left column*) and comparison to variability-based approach for obtaining the robot stiffness (*right column*). The *top left graph* shows the position trajectory of robot end-effector in *y-axis* (along the groove). The *middle left graph* shows the position trajectory in *z-axis* (vertical). The *bottom left graph* shows the stiffness trajectory. The *blue lines* in the *left column graphs* correspond to the trajectories formed from the demonstrated training data, while the *red lines* correspond to the learnt DMP trajectories. The *top right graph* shows the trajectories in *x-axis* (perpendicular to the groove), where *blue lines* represent trajectories from multiple teaching repetitions, *solid red line* represents their mean and *shaded red area* represents their variability. The *bottom right graph* shows the stiffness trajectory obtained from the inverse of variability of position trajectories (Color figure online)

the stiffness can be kept low (i.e. as in the strategy directly demonstrated through the proposed approach).

After the learning stage was finished, we used the strategy obtained by the proposed approach and made the robot execute the demonstrated task autonomously (see photos in the second column of Fig. 4). The learnt trajectories were controlled by a phase input signal described by (9). During this process we can control the speed of the task execution by changing the frequency of the phase signal. In this experiment we demonstrated the ability to arbitrarily change the task execution speed by switching between the three different task periods: 6, 10 and 18 s (frequency: 0.0556, 0.1 and 0.16667 Hz). The results of this experiment are shown in Fig. 6. The top graph shows the modulated execution frequency. The two graphs in the middle show the measured robot end-effector position in y and z-axes. The bottom graph shows the commanded robot stiffness.

We controlled the phase of DMPs to make a stop at the point where the bolt fitting should be tightened to fix the two parts together. The stopping point was time-independent and was determined by the phase; therefore the fixation point was uniquely and precisely defined with respect to the position. The results of this experiment can be observed in Fig. 7. The trajectory was reproduced at a predefined execution frequency 0.1 Hz. The frequency was set to 0 Hz at the phase where the robot reached the point of bolt fixation. This phase was set to $\frac{6\pi}{5}$. The phase control signal frequency was then kept at 0 Hz for 5 s for the purpose of tightening the bolt. After that, the trajectory execution was resumed by setting the frequency back to the execution frequency 0.1 Hz.

To demonstrate the advantage of low robot stiffness while the bolt is sliding inside the groove, we perturbed the base part by manually displacing it. With this we emulated instances such as human–robot cooperation and unpredictable events that may occur in real-world scenarios. In the first trial we used the stiffness as demonstrated by the tutor, i.e. high stiffness during the movement of the part in the air and lower stiffness while sliding the bolt inside the groove (see Fig. 8, lower left graph). In the second trial we used a preset constant high stiffness at the point of the perturbation (see Fig. 8, lower right graph), which also corresponds to the strategy obtained by the variability-based approach.

By observing the relations between the displacement of the end-effector position from the commanded reference position (Fig. 8, first row) and the resulting forces (Fig. 8, second row), we can see that the preset high stiffness produced relatively high forces even in case of small positional displacements. Exposing such system to strong perturbations

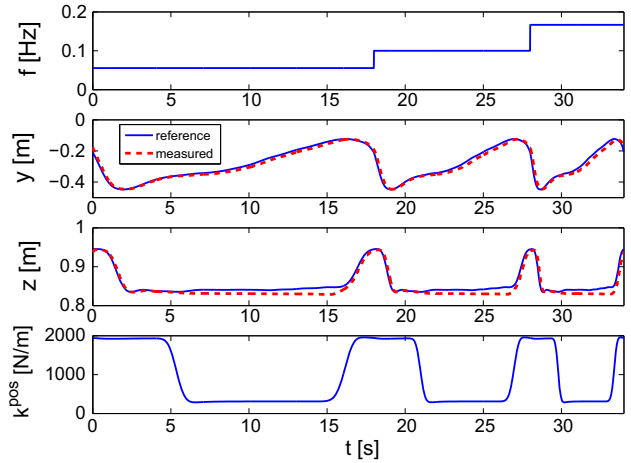

Fig. 6 Result of task execution speed adjustment. The *first graph* shows the commanded frequency. The *second graph* shows the measured robot end-effector *y-axis* position trajectory. The *third graph* shows the measured *z-axis* position trajectory. The *last graph* shows the commanded stiffness trajectory

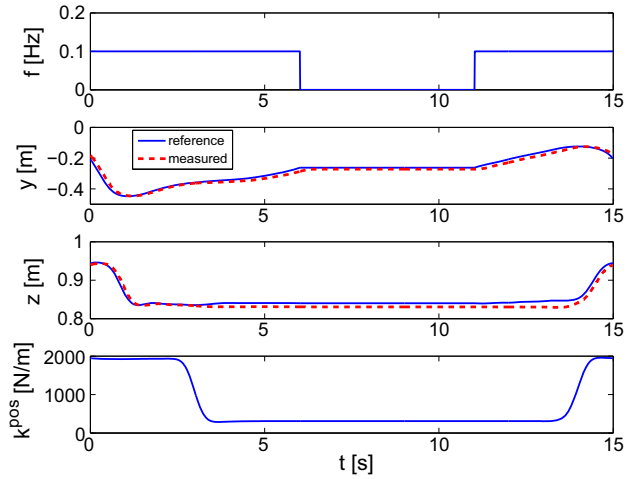

Fig. 7 Result of assembly task execution where phase was halted for purpose of bolt fixation. The *first graph* shows the commanded frequency. The *second graph* shows the measured robot end-effector position trajectory in the *y-axis*. The *third graph* shows the measured position trajectory in the *z-axis*. The *last graph* shows the commanded stiffness trajectory

could lead to equipment damage. In several occasions, the high interaction force resulted in bolt being stuck inside the groove. In contrast, robot produced relatively low interaction forces for the same level of positional displacements when the robot used the demonstrated low stiffness. Such method offers much safer operational conditions for the autonomous task production in an unpredictable environment or in the human–robot cooperation scenario.

At this point we should highlight several cases when the learnt behaviour can fail to produce the desired task. We examined some of these cases experimentally (see Online

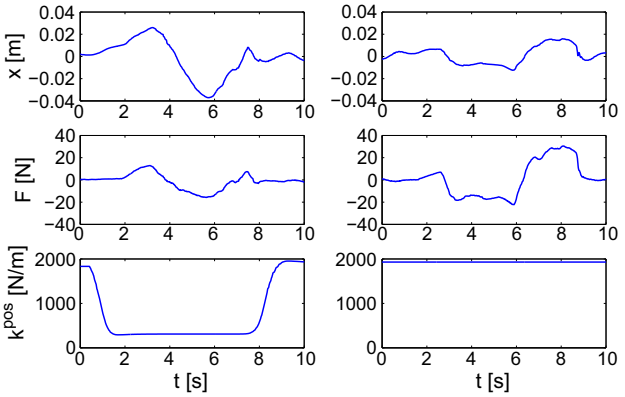

Fig. 8 Result of perturbation experiment for demonstrated variable robot stiffness (*left column*) and preset high stiffness (*right column*). The *top row graphs* show the displacement of robot end-effector *x-axis* position from the commanded reference position. The *middle row graphs* show the measured force in *x-axis* as a result of perturbation. The *bottom row graphs* show the commanded stiffness

Resource 2 for video). A failure with respect to the desired motion tracking can occur if an external perturbation produces a condition (e.g., displacement of the part on the table) where the friction between the tool (bolt, etc.) and the environment (groove, etc.) is higher than the force produced by the robot at the given instance. This failure condition can be formally expressed as

$$\boldsymbol{F}_{ext}(t) = \boldsymbol{K}\big(\boldsymbol{x}_d(t) - \boldsymbol{x}_a(t)\big) < \boldsymbol{F}_{frict}(t, \boldsymbol{x}_a), \tag{19}$$

where $\boldsymbol{F}_{ext}$ is force produced by the robot at the end-effector and $\boldsymbol{F}_{frict}$ is the friction (or stiction) force of the interaction between the robot-manipulated tool and the environment. Generally, the friction force depends on the given conditions such as task specifics, time, actual position, tool, material properties, etc.

Another failure to produce the task can occur during the bolt-insertion segment of the task. As the proposed approach relies on the learnt feed-forward behaviour, the displaced part in the environment might prevent a successful insertion of the bolt inside the groove. The exact tolerance with respect to the displacement from the learnt position depends on several factors. The insertion should be successful if the bolt surface is still within the groove surface. If the surface of the bolt goes outside the groove width due to the perturbation displacement then the bolt will be in contact with the edge of the groove. The successful insertion can then depend on the amount of the robot-produced force in the direction of the insertion and the passive elasticity of the bolt and groove material. For example, if the bolt or the groove material is very elastic, they can deform and make the insertion possible even in considerably displaced condition. On the other hand, if the material is very rigid, the two parts will get stuck and the robot will fail to execute the task.

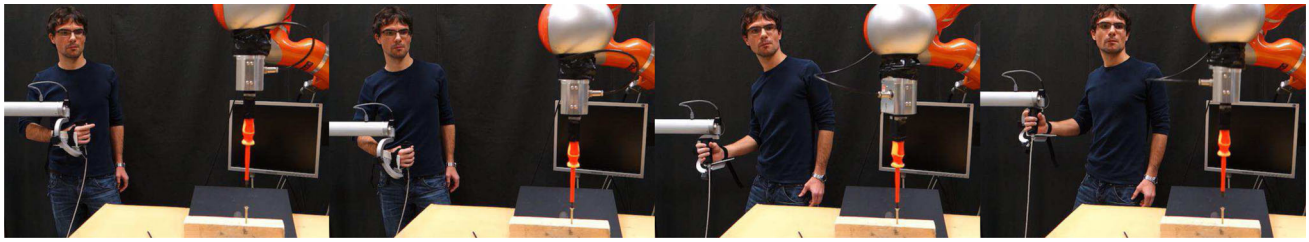

Fig. 9 Sequence of photos taken during the teaching stage of the bolt-screwing task

3.2 Self-tapping screw driving task

In the second series of experiments, we used the proposed teaching method to teach the robotic arm how to solve a bolt-screwing task. The course of the teaching stage is shown in Fig. 9. Please refer to Online Resource 1 for video of the experiment. The task involved driving the self-tapping screw with cross head into an un-modelled environment. The first step was to insert the screwdriver into the head of the bolt. This required motion in the z-axis of the work reference frame (see Fig. 10, top graph). We set the robot stiffness in z-axis to $k_z = 500\,\text{N/m}$ and kept it constant throughout the task. It was low enough to minimise the initial impact forces when the head of the screwdriver touched the head of the bolt. On the other hand, it was high enough to allow sufficient tracking of the robot end-effector position. The stiffness parameters in the x and y-axes were kept constant at 2000 N/m for this task.

The next step in the task was to fit the screwdriver into the screw head and rotate it for some angle to drive it into the material (see Fig. 10, middle graph). We devised a strategy that involved a variable rotational stiffness around z-axis. The tutor used stiffness control interface to change the rotational stiffness around the z-axis. At the point of inserting the screwdriver into the cross head of the screw, the rotational stiffness around the z-axis should ideally be low to simplify the insertion (see Fig. 10, bottom graph). Due to the unpredictable and unstructured environment, the bolt head and the screwdriver might not be perfectly aligned. In such cases low rotational stiffness allows the screwdriver to align to the current orientation of the bolt head and fit in. We set the maximum and minimum controllable rotational stiffness around z-axis to $k^{rotz}_{min} = 0\,\text{Nm/rad}$ and $k^{rotz}_{max} = 50\,\text{Nm/rad}$. The rotational stiffness in x and y-axes were kept constant at 200 Nm/rad for this task.

When the screwdriver was inserted into the bolt head, the tutor had to rotate the robot end-effector around z-axis. The rotation of tutor's arm was measured by *HapticMaster* gimbal device and was mapped to the robot end-effector rotation by factor 2. The tutor increased the rotational stiffness of the robot in order to achieve a good rotational tracking. The rotation could be potentially achieved at a very low rotational stiffness if the rotation reference was set at some large angle (i.e. further from the actual desired angle). If the environment was modelled then we would know what torque is required to drive the bolt into the material. By knowing the desired torque, one could calculate the necessary offset of reference orientation from actual orientation to produce that torque. However, in our case we did not know the model of the environment. Using the proposed teaching approach, we can compensate for the unstructured environment. The tutor was able to command high rotational stiffness through the stiffness control interface to make the robot strictly follow the reference rotation during the turn. Strict tracking of the reference rotation also simplified the screwdriver insertion in the next period as the bolt head was more precisely aligned.

When the bolt was rotated to the right for the desired angle, the stiffness was again reduced to simplify the withdrawal of the screwdriver from the bolt head. When the screwdriver was outside of the head, the tutor rotated the robot around the z-axis back to the left for the same angle. After this point, the process can be periodically repeated to perform the given task.

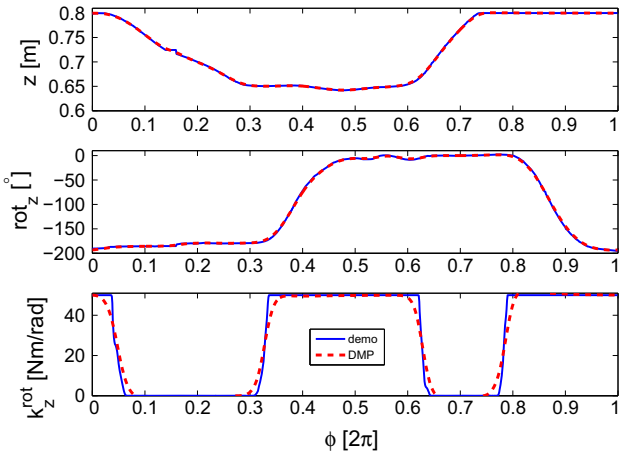

Fig. 10 Result of driving a self-tapping screw. The *top graph* shows the position trajectory of the robot end-effector in the *z-axis* (parallel to the screw). The *middle graph* shows the rotation trajectory along the *z-axis*. The *bottom graph* shows the rotational stiffness trajectory along the *z-axis*. The *blue lines* correspond to the trajectory formed from the demonstrated training data, while the *red lines* correspond to the learnt DMP trajectory (Color figure online)

During the demonstration stage, we collected the commanded position, rotation and stiffness variables. After the demonstration stage we used that data to make the phase-normalised trajectories and encoded them with periodic DMPs. The rotation around the z-axis was directly encoded with the DMP and transformed into the rotation matrix in the robot controller. This was possible since the task did not require to change the orientation around the other two axes simultaneously. If the task requires rotation around more than one axis then the orientation can be encoded with DMP where the parameters are learnt with locally weighted regression. The results of the learning process are presented in Fig. 10. The blue lines show the measured trajectories as commanded by the tutor and red lines show corresponding DMPs.

The learnt trajectories were then used in the autonomous stage where the robot performed the task autonomously. The trajectories were controlled by a phase input signal described by (9). Results of the autonomous operation are shown in Fig. 11. In the first graph there are the commanded reference robot motion (blue line) and the actual robot motion (red line) in the z-axis. We can see that the actual robot motion is gradually shifting in the direction of the negative z-axis as the screw in drilling into the material. The second graph shows the measured force in the z-axis. In the third graph of Fig. 11, there is the commanded reference rotation (blue line) and measure rotation (red line) around the z-axis. We can see that the robot achieved a good tracking under the commanded rotational stiffness (forth graph).

The force in the z-axis was slowly decreasing when the bolt was being driven into the material as a result of the constant commanded reference. The tutor commanded the reference deep enough to ensure the sufficient robot force in the z-axis throughout the task. A simple feedback algorithm could be implemented to maintain a constant force by adjusting the learnt reference based on the contact with the bolt and last measured position of the bolt. However, this was not necessary to complete the task. The proposed approach offers some degree of robustness to such variation.

A possible failure of the task may occur if the bolt head is displaced considerably from the learnt position in the x–y plane. In such case, the screwdriver can miss the bolt head during the approach. See Online Resource 2 for a video of this case. To deal with such cases, a visual feedback could be included in the autonomous robot control to readjust the learnt position when necessary.

4 Discussion

In the proposed method the human directly sets the impedance control strategy of the robot by commanding the stiffness trajectory. In contrast, some learning techniques use the variability of human-demonstrated motion trajectories to estimate the impedance of the robot (Calinon et al. 2010; Lee and Ott 2011; Kormushev et al. 2011; Paraschos et al. 2013). These studies suggest that the impedance should be low if the demonstrated trajectories have high variability, while the impedance should be high if the demonstrated trajectories have low variability. This method can provide a very good solution for many manipulation tasks and its advantage is that the human does not need to demonstrate the impedance separately. However, in some of the tasks involving physical interaction, such as slide-in-the-groove task, low trajectory variability does not necessarily correspond to the high impedance. As we shown in our experiments (Sect. 3.1), the impedance can be low despite the low trajectory variability, because it results from the robot being stabilised and constrained by the environment. Therefore, in this particular case, allowing the tutor to directly modulate the impedance is advantageous.

Similarly, kinaesthetic interaction based methods to demonstrate the robot impedance (Kronander and Billard 2014) may not be applicable in tasks such as slide-in-the-groove task. If low impedance had to be demonstrated inside the groove, the robot end-effector would need to be wiggled. This however may not be possible due to the constraints imposed by the environment.

Giving the tutor an option to control the stiffness of the robot during the teaching, provides a redundancy in the force control. If the task demands the robot to produce a certain force onto the environment, this can be achieved by multiple combinations of commanded position and commanded stiffness. The tutor can then determine the best combination for a given task. As we showed with an analysis and experiment (Sect. 2.3), this redundancy can be exploited to stabilise the force-feedback setup. If the task does not impose constrains on the stiffness modulation, the tutor can perform it with low commanded stiffness and minimise the effect of induced motion as a result of the feedback force applied at the end-effector. However, sometimes this is not possible as the task solution may impose constraints on the commanded stiffness. For example, this is the case when high tracking precision is required, whether due to the potentially unstable environment (Burdet et al. 2001), or due to the unknown environment (e.g., rotation of the self-tapping screw).

With the proposed approach, the human can effectively teach the robot how to perform various feed-forward behaviours that involve physical interaction with the environment. If necessary, the learnt feed-forward behaviour can be augmented with the feedback control. The trajectories can be further coupled with adaptive oscillators, if the task requires phase or frequency adaptation to some task-related variable or some arbitrary external variable (Petrič et al. 2011; Peternel et al. 2014, 2016a).

A potential limitation of the current stiffness control interface is that it only has one degree of freedom. This means

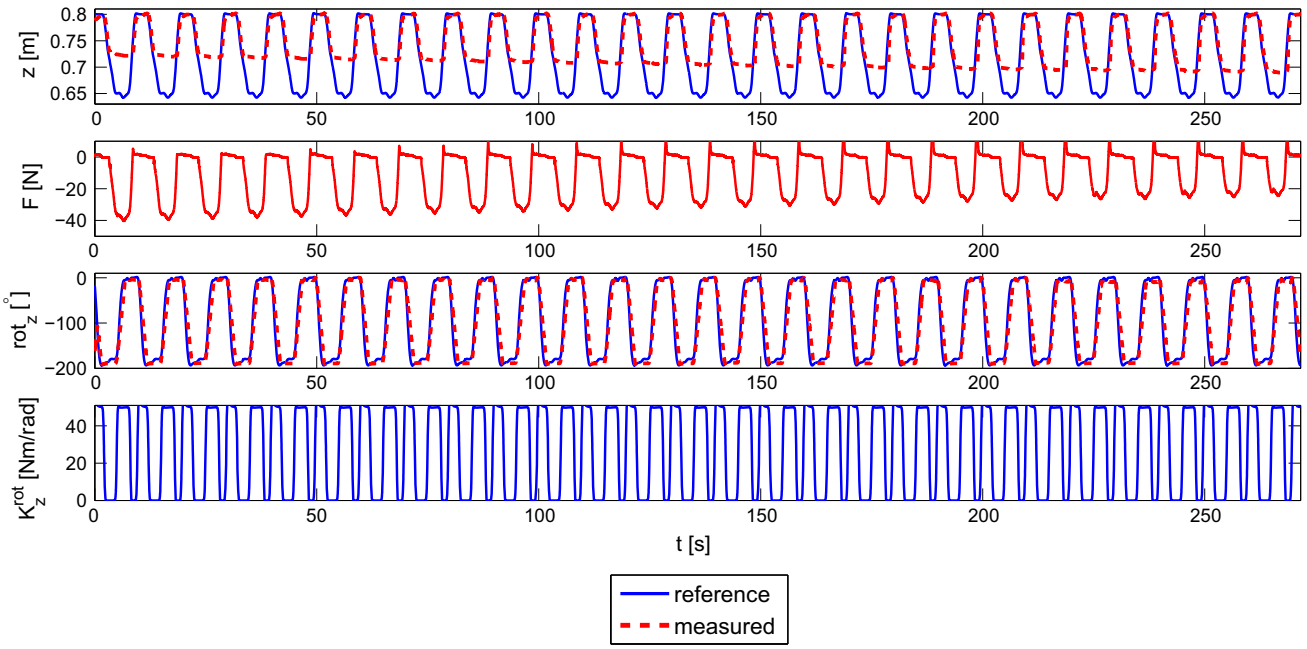

Fig. 11 Results of self-tapping screw driving task. The *first graph* shows the force in *z-axis* perpendicular to the object. The *second graph* shows the stiffness as modulated by the tutor. The *third graph* shows the displacement of the reference from the actual robot end-effector position along the *z-axis*

that the tutor can either change the robot stiffness in a single axis of the Cartesian space (e.g. as in the bolt-screwing task), or multiple axes at the same time (e.g. as in the slide-in-the-groove task). If the task requires more complex or independent multi-axis impedance regulation, human muscle activity based interface (Ajoudani et al. 2012) can be used in the proposed teaching framework. Alternatively, if the previously mentioned conditions (hazardous environment, task specifics, etc.) do not limit their application, complementary robot impedance teaching methods based on either kinaesthetic interaction (Kronander and Billard 2014), variability in demonstrated motion (Calinon et al. 2010; Lee and Ott 2011; Kormushev et al. 2011; Paraschos et al. 2013; Rozo et al. 2015) or iterative improvements (Yang et al. 2011; Buchli et al. 2011) can be used instead.

5 Conclusion

We proposed a human-in-the-loop method for teaching robots how to solve assembly tasks involving interaction with the environment. Classical end-effector force-feedback teleoperation setup was complemented with a novel stiffness control interface based on a linear spring-return potentiometer. We used the proposed method to teach the robot how to perform various assembly tasks. The collected training data was used to construct trajectories, which were used to reproduce the demonstrated actions in the autonomous stage. The key advantage of the proposed robot teaching setup is its intuitive application. Compared to the established manual programming, it offers significantly easier and faster means to teach the robot various complex skills. Through the experimental analyses and comparison, we demonstrated the advantages of directly teaching the robot how to modulate stiffness compared to the complementary methods.

Acknowledgements The authors would like to thank Barry Ridge for narrating the supplementary video.

References

Ajoudani, A., Godfrey, S., Bianchi, M., Catalano, M., Grioli, G., Tsagarakis, N., et al. (2014). Exploring teleimpedance and tactile feedback for intuitive control of the pisa/iit softhand. *IEEE Transactions on Haptics*, *7*(2), 203–215.

Ajoudani, A., Tsagarakis, N. G., & Bicchi, A. (2012). Tele-impedance: Teleoperation with impedance regulation using a body–machine interface. *The International Journal of Robotics Research*, *31*(13), 1642–1656.

Albu-Schäffer, A., Ott, C., Frese, U., & Hirzinger, G. (2003). Cartesian impedance control of redundant robots: Recent results with the DLR-light-weight-arms. In *2003 IEEE international conference on robotics and automation (ICRA)*, vol. 3, pp. 3704–3709.

Albu-Schäffer, A., Ott, C., & Hirzinger, G. (2007). A unified passivity-based control framework for position, torque and impedance control of flexible joint robots. *The International Journal of Robotics Research*, *26*(1), 23–39.

Argall, B. D., Chernova, S., Veloso, M., & Browning, B. (2009). A survey of robot learning from demonstration. *Robotics and Autonomous Systems*, *57*(5), 469–483.

Babič, J., Hale, J. G., & Oztop, E. (2011). Human sensorimotor learning for humanoid robot skill synthesis. *Adaptive Behavior—Animals, Animats, Software Agents, Robots, Adaptive Systems*, *19*, 250–263.

Ben Amor, H., Berger, E., Vogt, D., & Jung, B. (2009). Kinesthetic bootstrapping: Teaching motor skills to humanoid robots through physical interaction. In *Proceedings of the 32nd Annual German conference on advances in artificial intelligence*, pp. 492–499.

Ben Amor, H., Neumann, G., Kamthe, S., Kroemer, O., & Peters, J. (2014). Interaction primitives for human–robot cooperation tasks. In *2014 IEEE international conference on robotics and automation (ICRA)*, pp. 2831–2837.

Billard, A., Calinon, S., Dillmann, R., & Schaal, S. (2008). Robot programming by demonstration. In B. Siciliano & O. Khatib (Eds.), *Springer handbook of robotics* (pp. 1371–1394). Berlin: Springer.

Buchli, J., Stulp, F., Theodorou, E., & Schaal, S. (2011). Learning variable impedance control. *The International Journal of Robotics Research*, *30*(7), 820–833.

Burdet, E., Osu, R., Franklin, D. W., Milner, T. E., & Kawato, M. (2001). The central nervous system stabilizes unstable dynamics by learning optimal impedance. *Nature*, *414*(6862), 446–449.

Calinon, S., Sardellitti, I., & Caldwell, D. (2010). Learning-based control strategy for safe human–robot interaction exploiting task and robot redundancies. In *2010 IEEE/RSJ international conference on intelligent robots and systems (IROS)*, pp. 249–254.

Daniel, R., & McAree, P. (1998). Fundamental limits of performance for force reflecting teleoperation. *The International Journal of Robotics Research*, *17*(8), 811–830.

De Luca, A., Albu-Schäffer, A., Haddadin, S., & Hirzinger, G. (2006). Collision detection and safe reaction with the DLR-III lightweight manipulator arm. In *2006 IEEE/RSJ international conference on intelligent robots and systems (IROS)*, pp. 1623–1630.

Emge, N., Prebeg, G., Uygur, M., & Jaric, S. (2013). Effects of muscle fatigue on grip and load force coordination and performance of manipulation tasks. *Neuroscience Letters*, *550*, 46–50.

Evrard, P., Gribovskaya, E., Calinon, S., Billard, A., & Kheddar, A. (2009). Teaching physical collaborative tasks: Object-lifting case study with a humanoid. In *IEEE-RAS international conference on humanoid robots*, pp. 399–404.

Fite, K. B., Speich, J. E., & Goldfarb, M. (2001). Transparency and stability robustness in two-channel bilateral telemanipulation. *Journal of Dynamic Systems, Measurement, and Control*, *123*(8), 400–407.

Garabini, M., Passaglia, A., Belo, F., Salaris, P., & Bicchi, A. (2011). Optimality principles in variable stiffness control: The vsa hammer. In *2011 IEEE/RSJ international conference on intelligent robots and systems (IROS)*, pp. 3770–3775.

Hannaford, B., & Anderson, R. (1988). Experimental and simulation studies of hard contact in force reflecting teleoperation. In *1988 IEEE international conference on robotics and automation (ICRA)*, (pp. 584–589). Philadelphia, USA.

Hersch, M., Guenter, F., Calinon, S., & Billard, A. (2008). Dynamical system modulation for robot learning via kinesthetic demonstrations. *IEEE Transactions on Robotics*, *24*(6), 1463–1467.

Hogan, N. (1984). Adaptive control of mechanical impedance by coactivation of antagonist muscles. *IEEE Transactions on Automatic Control*, *29*(8), 681–690.

Hogan, N. (1985). Impedance control: An approach to manipulation. I—Theory. II—Implementation. III—Applications. *ASME Transactions Journal of Dynamic Systems and Measurement Control B*, *107*, 1–24.

Ijspeert, A. J., Nakanishi, J., Hoffmann, H., Pastor, P., & Schaal, S. (2013). Dynamical movement primitives: Learning attractor models for motor behaviors. *Neural Computation*, *25*(2), 328–373.

Ijspeert, A. J., Nakanishi, J., & Schaal, S. (2002a). Learning rhythmic movements by demonstration using nonlinear oscillators. In *2002 IEEE/RSJ international conference on intelligent robots and systems (IROS)*, pp. 958–963.

Ijspeert, A . J., Nakanishi, J., & Schaal, S. (2002b). Movement imitation with nonlinear dynamical systems in humanoid robots. In *2002 IEEE international conference on robotics and automation (ICRA)*, vol. 2, pp. 1398–1403.

Imamizu, H., Miyauchi, S., Tamada, T., Sasaki, Y., Takino, R., Pütz, B., et al. (2000). Human cerebellar activity reflecting an acquired internal model of a new tool. *Nature*, *403*(6766), 192–195.

Kawato, M. (1999). Internal models for motor control and trajectory planning. *Current Opinion in Neurobiology*, *9*(6), 718–727.

Kim, W., Hannaford, B., & Fejczy, A. (1992). Force-reflection and shared compliant control in operating telemanipulators with time delay. *IEEE Transactions on Robotics and Automation*, *8*(2), 176–185.

Kober, J., Wilhelm, A., Oztop, E., & Peters, J. (2012). Reinforcement learning to adjust parametrized motor primitives to new situations. *Autonomous Robots*, *33*(4), 361–379.

Kormushev, P., Calinon, S., & Caldwell, D. (2010). Robot motor skill coordination with em-based reinforcement learning. In *2010 IEEE/RSJ international conference on intelligent robots and systems (IROS)*, pp. 3232–3237.

Kormushev, P., Calinon, S., & Caldwell, D. G. (2011). Imitation learning of positional and force skills demonstrated via kinesthetic teaching and haptic input. *Advanced Robotics*, *25*(5), 581–603.

Kronander, K., & Billard, A. (2012). Online learning of varying stiffness through physical human–robot interaction. In *2012 IEEE international conference on robotics and automation (ICRA)*, pp. 1842–1849.

Kronander, K., & Billard, A. (2014). Learning compliant manipulation through kinesthetic and tactile human–robot interaction. *IEEE Transactions on Haptics*, *7*(3), 367–380.

Kronander, K., Burdet, E., & Billard, A. (2014). Task transfer via collaborative manipulation for insertion assembly. *Workshop on human–robot interaction for industrial manufacturing, robotics, science and systems*.

Kuchenbecker, K. J., & Niemeyer, G. (2006). Induced master motion in force-reflecting teleoperation. *Journal of Dynamic Systems, Measurement, and Controlh*, *128*(4), 800–810.

Kushida, D., Nakamura, M., Goto, S., & Kyura, N. (2001). Human direct teaching of industrial articulated robot arms based on force-free control. *Artificial Life and Robotics*, *5*(1), 26–32.

Lee, D., & Ott, C. (2011). ncremental kinesthetic teaching of motion primitives using the motion refinement tube. *Autonomous Robots*, *31*(2), 115–131.

Liang, P., Yang, C., Li, Z., & Li, R. (2015). Writing skills transfer from human to robot using stiffness extracted from sEMG. In *2015 IEEE international conference on cyber technology in automation, control, and intelligent systems (CYBER)*, pp. 19–24.

Oztop, E., Lin, L.-H., Kawato, M., & Cheng, G. (2006). Dexterous skills transfer by extending human body schema to a robotic hand. In *2006 6th IEEE-RAS international conference on humanoid robots*, pp. 82–87.

Paraschos, A., Daniel, C., Peters, J., & Neumann, G. (2013). Probabilistic movement primitives. In C. Burges, L. Bottou, M. Welling, Z. Ghahramani, & K. Weinberger (Eds.), *Advances in neural information processing systems 26* (pp. 2616–2624). Red Hook: Curran Associates Inc.

Peternel, L., Noda, T., Petrič, T., Ude, A., Morimoto, J., & Babič, J. (2016a). Adaptive control of exoskeleton robots for periodic assistive behaviours based on EMG feedback minimisation. *PLoS ONE*, *11*(2), e0148942.

Peternel, L., Petrič, T., & Babič, J. (2015). Human-in-the-loop approach for teaching robot assembly tasks using impedance control interface. In *2015 IEEE international conference on robotics and automation (ICRA)*, pp. 1497–1502.

Peternel, L., Petrič, T., Oztop, E., & Babič, J. (2014). Teaching robots to cooperate with humans in dynamic manipulation tasks based on multi-modal human-in-the-loop approach. *Autonomous robots*, *36*(1–2), 123–136.

Peternel, L., Tsagarakis, N., & Ajoudani, A. (2016b). Towards multi-modal intention interfaces for human–robot co-manipulation. In *2016 IEEE/RSJ international conference on intelligent robots and systems (IROS)*, pp. 2663–2669.

Petrič, T., Gams, A., Ijspeert, A. J., & Žlajpah, L. (2011). On-line frequency adaptation and movement imitation for rhythmic robotic tasks. *The International Journal of Robotics Research*, *30*(14), 1775–1788.

Rozo, L., Bruno, D., Calinon, S., & Caldwell, D. G. (2015). Learning optimal controllers in human-robot cooperative transportation tasks with position and force constraints. In *2015 IEEE/RSJ international conference on intelligent robots and systems (IROS)*.

Schaal, S., & Atkeson, C. G. (1998). Constructive incremental learning from only local information. *Neural Computation*, *10*(8), 2047–2084.

Schindlbeck, C., & Haddadin, S. (2015). Unified passivity-based cartesian force/impedance control for rigid and flexible joint robots via task-energy tanks. In *2015 IEEE international conference on robotics and automation (ICRA)*, pp. 440–447.

Theodorou, E., Buchli, J., & Schaal, S. (2010). A generalized path integral control approach to reinforcement learning. *Journal of Machine Learning Research*, *11*, 3137–3181.

Todd, G., Gandevia, S. C., & Taylor, J. L. (2010). Change in manipulation with muscle fatigue. *European Journal of Neuroscience*, *32*(10), 1686–1694.

Tonietti, G., Schiavi, R., & Bicchi, A. (2005). Design and control of a variable stiffness actuator for safe and fast physical human/robot interaction. In *2005 IEEE international conference on robotics and automation (ICRA)*, pp. 526–531.

Tsumugiwa, T., Yokogawa, R., & Hara, K. (2002). Variable impedance control with virtual stiffness for human-robot cooperative peg-in-hole task. In *2002 IEEE/RSJ international conference on intelligent robots and systems (IROS)*, vol. 2, pp. 1075–1081.

Van Der Linde, R. Q., Lammertse, P., Frederiksen, E., & Ruiter, B. (2002). The hapticmaster, a new high-performance haptic interface. In *Proceedings of Eurohaptics, 2002*, 1–5.

Walker, D., Salisbury, J., & Niemeyer, G. (2011). Demonstrating the benefits of variable impedance to telerobotic task execution. In *IEEE international conference on robotics and automation (ICRA), 2011* , (pp. 1348–1353).

Walker, D., Wilson, R., & Niemeyer, G. (2010). User-controlled variable impedance teleoperation. In *IEEE International Conference on Robotics and Automation (ICRA), 2010* , (pp. 5352–5357).

Wolf, S., & Hirzinger, G. (2008). A new variable stiffness design: Matching requirements of the next robot generation. In *IEEE International Conference on Robotics and Automation (ICRA), 2008*, (pp. 1741–1746).

Wolpert, D. M., Miall, R. C., & Kawato, M. (1998). Internal models in the cerebellum. *Trends in Cognitive Sciences*, *2*(9), 338–347.

Yang, C., Ganesh, G., Haddadin, S., Parusel, S., Albu-Schäffer, A., & Burdet, E. (2011). Human-like adaptation of force and impedance in stable and unstable interactions. *IEEE Transactions on Robotics*, *27*(5), 918–930.

Luka Peternel graduated from University of Ljubljana, Slovenia in 2011. He received his Ph.D. in robotics from University of Ljubljana in 2015. He was with Department of Automation, Biocybernetics and Robotics at Jožef Stefan Institute in Ljubljana from 2011 to 2015. He conducted a part of his Ph.D. research at BRI, ATR Computational Neuroscience Laboratories in Kyoto, Japan during 2013 and 2014. From October 2015 he is a postdoctoral researcher at HRI^2 lab, Advanced Robotics, Italian Institute of Technology in Genoa, Italy. His main research topics are human-in-the-loop robot control and learning, physical human-robot interaction and exoskeleton control.

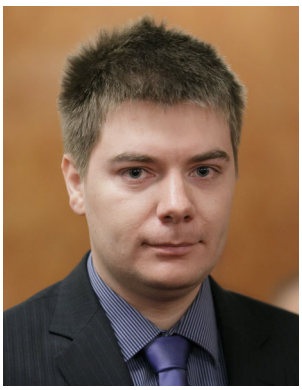

Tadej Petrič attended the University of Maribor, Slovenia, where he obtained an M.Sc. in Electrical Engineering in 2008. His M.Sc. covered modeling and robotic control of underactuated dynamic system. For his work, he received the Prof. Dr. Vratislav Bedjanič award in 2008. In 2013 he received a D.Sc. in robotics from the Faculty of Electrical Engineering at the University of Ljubljana. He performed a part of his doctoral research at the Department of Robotic Systems for Dynamic Control of Legged Humanoid Robots at the German Aerospace Center (DLR) in Oberpfaffenhofen, Germany. In 2013, he was a visiting researcher at ATR Computational Neuroscience Laboratories in Japan. In 2015, he was a Postdoctoral Fellow in the Biorobotics Laboratory at the Swiss Federal Institute of Technology (EPFL) in Lausanne, Switzerland. He is currently a researcher at Jozef Stefan Institute in Ljubljana, Slovenia. His current research is concerned with the design of biologically plausible robot controllers that achieve robustness and adaptation to changing environments comparable to that found in humans.

Jan Babič is a Senior Researcher at Jožef Stefan Institute, Slovenia and an Assistant Professor at Faculty of Electrical Engineering, University of Ljubljana, Slovenia. He received his Ph.D. examining the role of biarticular muscles in human locomotion. During the years 2006/2007 he was a visiting researcher at ATR Computational Neuroscience Laboratories in Japan. In November 2014 he was a visiting professor at The Institute for Intelligent Systems and Robotics, University of Pierre and Marie Curie in France. His current research is particularly concerned with the understanding how human brain controls movement of the body. He is using these neurophysical models to design biologically plausible solutions for a broad spectrum of robotic systems such as industrial robots, humanoids, exoskeletons and rehabilitation devices.